Net Bitrate of >1.3-Tb/s/λ Transmission over 80 km with Transmitter-side Semiconductor Optical Amplifier

Fukutaro Hamaoka, Masanori Nakamura, Takeo Sasai, Takayuki Kobayashi, Yoshiaki Kisaka, and Yutaka Miyamoto

NTT Network Innovation Laboratories, Yokosuka, Japan, fukutaro.hamaoka@ntt.com

Abstract *We evaluated 144-GBaud 64QAM signal characteristics with transmitter-side SOA. Back-to-back experiments demonstrated up to 1.38-Tb/s/λ net bitrate with optimized SOA input powers and injection currents. We also performed 80-km SMF transmission between 1530.529 and 1564.067 nm, achieving >1.3-Tb/s/λ net bitrate with the optimum SOA conditions. ©2023 The Author(s)*

Introduction

The capacity of optical transmission systems has been steadily increasing, as helped by breakthroughs such as digital coherent technologies, to manage the rapid growth in communication traffic. Alongside, the capacity per wavelength (b/s/λ) of an optical transceiver must be expanded to achieve cost-effective systems and to accommodate the high-speed client signals of the next-generation Ethernet [1], such as 800 GbE, 1.6 TbE, and beyond. The highest capacity per wavelength, i.e., greater than 2 Tb/s/λ, has recently been demonstrated over 240-km transmission in the C-band [2]. Experimental demonstrations of 1.6 Tb/s/λ coherent transmission have also been reported in the O-band over 10 km [3] and in the C-band over 81 km with 16 channels [4].

As the capacity of optical transmission systems has increased, it has become necessary to utilize smaller form factors, such as the integrated coherent transmit-receiver optical subassembly (IC-TROSA) [5], to reduce the power consumption of coherent transceivers with high capacity per wavelength. A key component in integrated coherent transceivers is a semiconductor optical amplifier (SOA) thanks to its small size and low power consumption. Since SOAs also offer high flexibility in designing the amplification band, they have been applied to optical transmission lines in experiments for 5-band [6] and 3-band [7] wavelength division multiplexing configurations. It has also been reported that SOAs were used as a transmitter booster and receiver pre-amplifier in an IC-TROSA configuration for 400-Gb/s/λ and 600-Gb/s/λ applications with 64-GBaud 16 quadrature amplitude modulation (QAM) and 64QAM signals [8]. We previously proposed an SOA-integrated ultra-broadband transmitter configuration with analogue multiplexing function [9]. Our experiments indicated that the SOA was able to be applied to the 1-Tb/s/λ signal with 168-GBuad polarization-multiplexed (PDM) probabilistic-constellation-shaped (PCS) 16QAM by suppressing the signal-to-noise ratio (SNR) penalty caused by the SOA-induced nonlinear distortion to less than 1 dB.

In this study, we experimentally evaluate the applicability of a high-symbol rate signal with a high-order modulation format, i.e., a 144-GBaud 64QAM signal, to an SOA-integrated transmitter configuration. In back-to-back experiments, the net bitrate of up to 1.38 Tb/s/λ was demonstrated at a centre carrier wavelength of 1547.116 nm with optimal SOA input powers and SOA injection currents. We also performed 80-km single-mode fibre (SMF) transmission in the C-band with the transmitter-side SOA. The 80-km SMF transmission results demonstrated that the net bitrate of >1.3-Tb/s/λ was achieved with optimum SOA input powers and SOA injection currents in the C-band covering between 1530.529 and 1564.067 nm.

Experimental Setup

Figure 1(a) shows the experimental setup for following an SOA-integrated transmitter configuration. Offline transmitter-side digital signal processing (Tx-DSP) prepared the high-

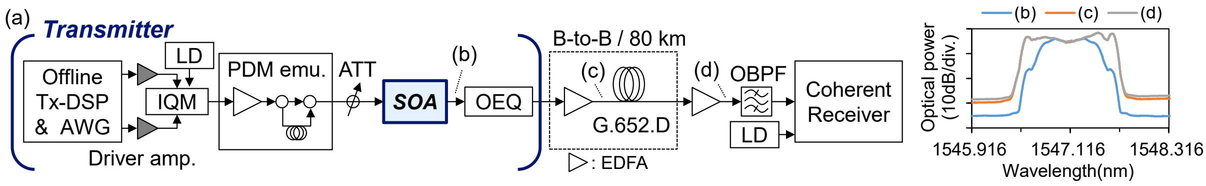

Fig. 1: (a) Experimental setup for evaluating back-to-back and 80-km transmission characteristics of 144-GBaud PCS-64QAM signal using transmitter-side SOA, and optical spectra (b) output from SOA, (c) applied with OEQ (before 80-km transmission), and (d) after 80-km transmission.

symbol-rate 144-GBaud signals by applying a third-order Volterra filter to compensate for the nonlinearity of driver amplifiers [10] and a root-raised-cosine filter with a roll-off factor of 0.3 for up-sampling. The high-symbol-rate signals were then output from a 256-GSa/s 70-GHz-bandwidth (BW) arbitrary waveform generator (AWG). The electrical signals from the 67-GHz-BW driver amplifiers were modulated in a 20-GHz-BW lithium niobate IQ modulator (IQM) with an optical carrier from a laser diode (LD) source of an external cavity laser. A PDM 144-GBaud PCS-64QAM signal was output from a PDM emulator consisting of an erbium-doped fibre amplifier (EDFA), polarization beam combiners, and a delay line. Then, the signal was amplified by an SOA. The input power to the SOA was controlled by a variable optical attenuator (ATT). The frequency amplitude response of the high-symbol-rate 144-GBaud signal output from the SOA (see Fig. 1(b)) was compensated with an optical equalizer (OEQ) based on an optical flexible-grid wavelength selective switch as shown in Fig. 1(c).

The performance of the 144-GBaud PCS-64QAM signal was evaluated both in a back-to-back configuration and after 80-km transmission through SMF which is compliant with ITU-T G.652.D. The centre carrier wavelength of the measured signal in the C-band was set to 1547.116 nm in the back-to-back and 1530.529, 1538.778, 1547.116, 1555.545, and 1564.067 nm in the 80-km transmission experiments. The loss coefficient of the optical transmission line was 0.187 dB/km at 1547.116 nm in this experiment. The fibre-launched power from an EDFA was set to 7 dBm. The optical spectrum after 80-km transmission is shown in Fig. 1(d). The received signal through an optical bandpass filter (OBPF) was detected using a coherent receiver with an optical local oscillator which was an LD source of an integrable tunable laser assembly. The coherent receiver consisted of an optical 90-degree hybrid, four 100-GHz-BW balanced photodetectors, a 256-GSa/s 113-GHz-BW digital storage oscilloscope, and an offline receiver-side (Rx) DSP.

In the offline RX-DSP, the Tx- and Rx-linear responses and the carrier phase of the received 144-GBaud PCS-64QAM signal were simultaneously compensated by a frequency domain 8×2 MIMO adaptive equalizer [11] with a pilot-based digital phase-locked loop using the pilot QPSK symbol every 64-symbol duration. Then, a bit-metric decoder [12] calculated the log-likelihood ratios. We measured the SNR and the normalized generalized mutual information (NGMI) of the received signal. To enable a rate adaptive coding [13], a family of DVBS2 low-density parity-check (LDPC) codes [14] with a puncturing method [15] was used to determine the required code rate for error-free decoding, which assumes outer hard-decision FEC with a code rate of 0.9922 and BER threshold of 5×10^{-5} [16]. More than 1200 codewords were examined for LDPC decoding. The achievable and net bitrate of the received signal were calculated from the NGMI and required code rate, respectively, using the equation of $C = [2 \cdot \{H_{2D} - (1 - R) \cdot \log_2 M\} \cdot B] \,/\, (1 + P_{OH}/100)$, where H_{2D} is the constellation entropy per 2D symbol, R is the NGMI or code rate, M is the modulation order of the QAM, B is the symbol rate, and P_{OH} is the pilot overhead (OH). In this experiment, the entropy of the PCS-64QAM signal was 5.829 bit/2Dsymbol and the pilot OH was 1.5873%.

Results and Discussion

First, we evaluated how SOA-induced nonlinear distortion affects the signal characteristics, as shown in Fig. 2, under the back-to-back configuration for the 144-GBaud 64QAM signal. With increasing the SOA input power, the saturation characteristic of the SOA was observed from the output power and the SOA gain for each SOA injection current between 100

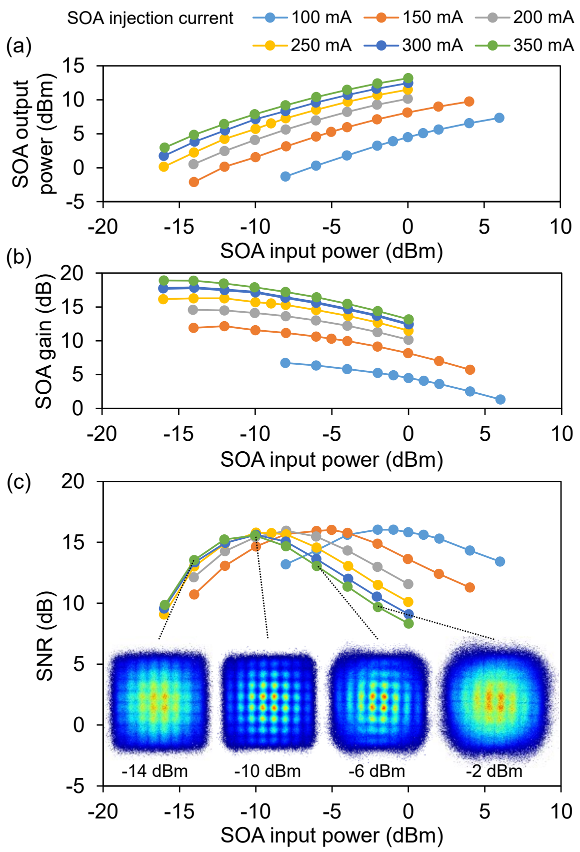

Fig. 2: Dependencies of SOA input power and SOA injection current on (a) SOA output power, (b) SOA gain, and (c) SNR measured in back-to-back configuration.

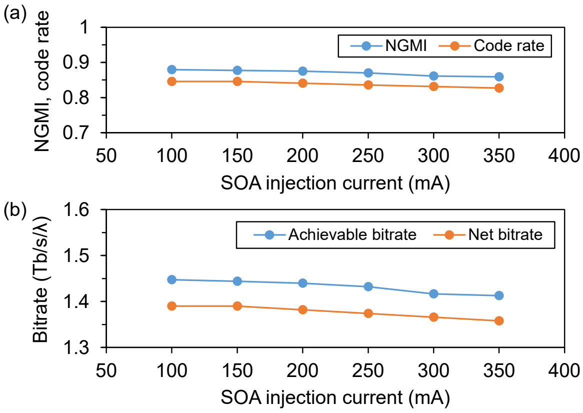

Fig. 3: Dependencies of SOA injection current on (a) NGMI and required code rate and (b) achievable and net bitrate at optimum SOA input power in back-to-back configuration.

and 350 mA, as shown in Fig. 2(a) and (b), respectively. The measured SNR for each SOA injection current is shown in Fig. 2(c) as a function of SOA input power. For example, in the case of the SOA injection current of 350 mA, the optimum SOA input power obtaining the highest SNR was -10 dBm. When the SOA input powers were lower than the optimum input power, the SNR degradation occurred with the decreased input powers, as shown in the constellation of Fig. 2(c) at the SOA input power of -14 dBm. In contrast, when the SOA input powers were higher than the optimum input power, the signal performances were degraded mainly due to the SOA-induced nonlinear distortion (see constellations in Fig. 2(c) at the SOA input powers of -6 and -2 dBm). Figure 3(a) shows the NGMI and the required code rate as a function of SOA injection current in the back-to-back

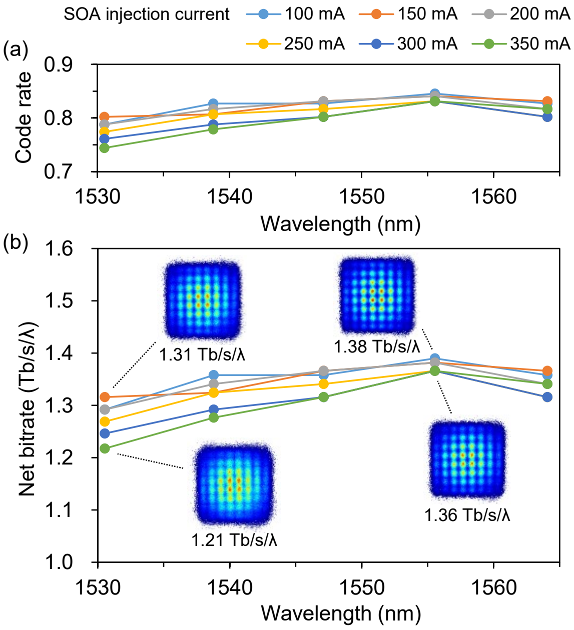

Fig. 4: Wavelength dependencies of 144-GBaud 64QAM signal after SFM transmission over 80-km on (a) code rate and (b) net bitrate in C-band for each SOA injection current.

configuration. The optimum SOA input powers obtaining maximum NGMI were -2 dBm at the injection current of 100 mA, -5 dBm at 150 mA, -8 dBm at 200 mA, and -10 dBm at 250, 300, and 350 mA. As shown in Fig. 3(b), the achievable bitrate was between 1.41 and 1.44 Tb/s/λ and the net bitrate was between 1.35 and 1.38 Tb/s/λ for each SOA injection current at the centre carrier wavelength of 1547.116 nm in the back-to-back experiments.

We also demonstrated the SMF transmission of the 144-GBaud PCS-64QAM signal over 80 km at the centre carrier wavelength of 1530.529, 1538.778, 1547.116, 1555.545, and 1564.067 nm, which covers the C-band. The signal was transmitted using the optimum SOA input power obtained from the back-to-back experiments. Figure 4 shows the wavelength dependencies of the 144-GBaud 64QAM signal after 80-km SMF transmission on (a) the required code rate and (b) the net bitrate for each SOA injection current. The net bitrate of the 144-GBaud PCS-64QAM signal was obtained from 1.21 and 1.38 Tb/s/λ under all conditions after the 80-km SMF transmission in the C band. Especially, the net bitrate ranged from 1.31 to 1.38 Tb/s/λ, when the optimum SOA input power and SOA injection current were selected for each wavelength.

Conclusion

We conducted experiments to evaluate the performance of a high-symbol-rate 144-GBaud 64QAM signal in an experimental setup that follows an SOA-integrated transmitter configuration. Back-to-back experiments were performed and a net bitrate between 1.35 and 1.38 Tb/s/λ at 1547.116 nm was achieved with the optimum SOA input power for each SOA injection current. Additionally, we performed an 80-km SMF transmission of the 144-GBaud 64QAM signal, achieving a net bitrate of >1.3-Tb/s/λ by selecting optimum SOA input powers and injection currents in the range of 1530.529 to 1564.067 nm in the C-band. The experimental demonstration indicates that the transmitter-side SOA is a promising configuration to achieve >1 Tb/s/λ signal transmission with a high-symbol rate and a high-order modulation format for the realization of a compact and low-power transmitter.

References

[1] Ethernet Alliance, "2023 Ethernet Roadmap," https://ethernetalliance.org/technology/ethernet-roadmap/

[2] M. Nakamura, M. Nagatani, T. Jyo, F. Hamaoka, M. Mutoh, Y. Shiratori, H. Wakita, T. Kobayashi, H. Takahashi, and Y. Miyamoto, "Over 2-Tb/s Net Bitrate

Single-carrier Transmission Based on >130-GHz-Bandwidth InP-DHBT Baseband Amplifier Module," in *Proceedings The European Conference on Optical Communication (ECOC)*, Basel, Switzerland, 2022, Th3C.1.

[3] E. Berikaa, M. S. Alam, S. Bernal, W. Li, B. Krueger, F. Pittalà, and D. V. Plant, "Net 1.6 Tbps O-band Coherent Transmission over 10 km Using a TFLN IQM and DFB Lasers for Carrier and LO," in *Proceedings Optical Fiber Communication Conference (OFC)*, San Diego, CA, USA, 2023, Th4B.1.

[4] D. Che, S. Grillanda, Y. Liu, Z. Qiu, X. Ji, G. Raybon, X. Chen, K. Kim, T. J. Kippenberg, and A. Blanco-Redondo, "First Demonstration of Erbium-Doped Waveguide Amplifier Enabled Multi-Tb/s (16×1.6T) Coherent Transmission," in *Proceedings Optical Fiber Communication Conference (OFC)*, San Diego, CA, USA, 2023, Th4B.3.

[5] OIF, "Integrated Coherent Transmit-Receive Optical Sub Assembly (IC-TROSA)," https://www.oiforum.com/technical-work/hot-topics/integrated-coherent-transmit-receive-optical-sub-assembly-ic-trosa/

[6] S. Okamoto, K. Horikoshi, F. Hamaoka, K. Minoguchi, and A. Hirano, "5-band (O, E, S, C, and L) WDM Transmission with Wavelength Adaptive Modulation Format Allocation," in *Proceedings The European Conference on Optical Communication (ECOC)*, Dusseldorf, Germany, 2016, Th.2.P2.SC5.4

[7] J. Renaudier, A. Carbo Meseguer, A. Ghazisaeidi, P. Tran, R. R. Muller, R. Brenot, A. Verdier, F. Blache, K. Mekhazni, B. Duval, H. Debregeas, M. Achouche, A. Boutin, F. Morin, L. Letteron, N. Fontaine, Y. Frignac, and G. Charlet, "First 100-nm Continuous-Band WDM Transmission System with 115Tb/s Transport over 100km Using Novel Ultra-Wideband Semiconductor Optical Amplifiers," in *Proceedings The European Conference on Optical Communication (ECOC)*, Gothenburg, Sweden, 2017, Th.PDP.A.3., DOI: 10.1109/ECOC.2017.8346084

[8] J. Zhou, L. Zhu, D. Wong, H. Wang, M. Boudreau, J. Sun, J. Huang, P. Wang, G. Ji, and J. Hong, "Characterizations of Semiconductor Optical Amplifiers for 64Gbaud 16-64QAM Coherent Optical Transceivers," in *Proceedings Optical Fiber Communication Conference (OFC)*, San Diego, CA, USA, 2019, Tu2H.7, DOI: 10.1364/OFC.2019.Tu2H.7

[9] F. Hamaoka, M. Nakamura, T. Kobayashi, M. Nagatani, H. Wakita, H. Yamazaki, Y. Ogiso, and Y. Miyamoto, "Experimental Investigation of Influence of SOA-Induced Nonlinear Distortion on High-Symbol-Rate 168-GBaud Signal for Achieving Ultra-Broadband Optical Frontend," in *Proceedings Optical Fiber Communication Conference (OFC)*, San Diego, CA, USA, 2022, M3H.2, DOI: 10.1364/OFC.2022.M3H.2

[10] P. W. Berenguer, M. Nölle, L. Molle, T. Raman, A. Napoli, C. Schubert, and J. K. Fischer, "Nonlinear Digital Pre-distortion of Transmitter Components," *Journal of Lightwave Technology*, vol. 34, no. 8, pp. 1739–1745, 2016, DOI: 10.1109/JLT.2015.2510962

[11] M. Nakamura, T. Kobayashi, F. Hamaoka, and Y. Miyamoto, "High Information Rate of 128-GBaud 1.8-Tb/s and 64- GBaud 1.03-Tb/s Signal Generation and Detection Using Frequency-Domain 8×2 MIMO Equalization," in *Proceedings Optical Fiber Communication Conference (OFC)*, San Diego, CA, USA, 2022, M3H.1, DOI: 10.1364/OFC.2022.M3H.1

[12] G. Böcherer, F. Steiner, and P. Schulte, "Bandwidth Efficient and Rate-Matched Low-Density Parity-Check Coded Modulation," *IEEE Transactions on Communications*, vol. 63, no. 12, pp. 4651–4665, 2015, DOI: 10.1109/TCOMM.2015.2494016

[13] A. Ghazisaeidi, L. Schmalen, I. F. de Jauregui Ruiz, P. Tran, C. Simonneau, P. Brindel, and G. Charlet "Transoceanic Transmission Systems Using Adaptive Multirate FECs," *Journal of Lightwave Technology*, vol. 33, no. 7, pp. 1479–1487, 2015, DOI: 10.1109/JLT.2015.2399174

[14] ETSI, EN 302 307-1, v.1.4.1, 2014.

[15] T. Yoshida, M. Karlsson, and E. Agrell, "Efficient Offline Evaluation of FEC Codes Based on Captured Data with Probabilistic Shaping," in *Proceedings Optical Fiber Communication Conference (OFC)*, San Diego, CA, USA, 2018, M4E.5, DOI: 10.1364/OFC.2018.M4E.5

[16] D.S. Millar, R. Maher, D. Lavery, T. Koike-Akino, M. Pajovic, A. Alvarado, M. Paskov, K. Kojima, K. Parsons, B.C. Thomsen, S.J. Savory, and P. Bayvel "Design of a 1 Tb/s Superchannel Coherent Receiver," *Journal of Lightwave Technology*, vol. 34, no. 6, pp. 1453–1463, 2016, DOI: 10.1109/JLT.2016.2519260